Preparation and performance of plastic scintillators with copper iodide complex-loaded for radiation detection

Wen Li, Yunyun Li, Martin Nikl, Matthieu Hamel, Hongshu Wu, Romana Kucerkova, Vladimir Babin, Guohao Ren, Yuntao Wu

▶ **To cite this version:**

Wen Li, Yunyun Li, Martin Nikl, Matthieu Hamel, Hongshu Wu, et al.. Preparation and performance of plastic scintillators with copper iodide complex-loaded for radiation detection. Polymer, 2022, 249, pp.124832. 10.1016/j.polymer.2022.124832 . cea-04155603

HAL Id: cea-04155603
https://cea.hal.science/cea-04155603v1

Submitted on 7 Jul 2023

HAL is a multi-disciplinary open access archive for the deposit and dissemination of scientific research documents, whether they are published or not. The documents may come from teaching and research institutions in France or abroad, or from public or private research centers.

L'archive ouverte pluridisciplinaire **HAL**, est destinée au dépôt et à la diffusion de documents scientifiques de niveau recherche, publiés ou non, émanant des établissements d'enseignement et de recherche français ou étrangers, des laboratoires publics ou privés.

Preparation and Performance of Plastic Scintillators with Copper Iodide Complex-loaded for Radiation Detection

Wen Li,[a,b,c] Yunyun Li,[a,b,*] Martin Nikl,[d] Matthieu Hamel,[e] Hongshu Wu,[a] Romana Kucerkova,[d] Vladimir Babin,[d] Guohao Ren,[a,b] Yuntao Wu [a,b,*]

[a] *Shanghai Institute of Ceramics, Chinese Academy of Sciences, 585 He-Shuo Road, Shanghai 201899, China*
[b] *State Key Laboratory of Intense Pulsed Radiation Simulation and Effect, Xi'an, 710024, China*
[c] *College of Materials and Chemistry, China Jiliang University, Hangzhou 310018, China*
[d] *Institute of Physics of the Czech Academy of Sciences, Cukrovarnicka 10/112, Prague,16200, Czech Republic*
[e] *Université Paris Saclay, CEA, List, F 91121 Palaiseau, France*

Corresponding author: E-mail: ytwu@mail.sic.ac.cn; liyunyun225@163.com.

ABSTRACT

Development of plastic scintillators loaded with low-cost phosphorescent sensitizer is currently an important topic toward enhancing the scintillation light yield for radiation detection applications. In this work, we report plastic scintillators loaded with deep-blue-emitting phosphorescent sensitizer $CuI(PPh_3)_2$(*t*-BuPy), where PPh_3 and *t*-BuPy stand for triphenylphosphine and 4-*tert*-butylpyridine, respectively. $CuI(PPh_3)_2$(*t*-BuPy)-loaded poly(vinyltoluene) plastic scintillators with a high optical transmittance of over 80% were synthesized via bulk polymerization method. The optical absorption, photoluminescence spectra and decay kinetics, and scintillation performance under X-ray, γ-ray, and α-particle excitation were comprehensively investigated. The scintillation yield was reduced with the increase of $CuI(PPh_3)_2$(*t*-BuPy) loading concentration. The physical mechanism and the role of the copper iodide complex in scintillation yield reduction are proposed.

Keywords:

Plastic scintillators; poly(vinyltoluene); Cu-based phosphorescent complex; radiation detection.

1. Introduction

Scintillators, as a core component of radiation detector, are capable of interacting with high-energy particles/rays and converting them into detectable photons ranging from ultraviolet (UV) to visible light [1-3]. They have been widely used for nuclear medical imaging, high-energy physics, nuclear physics, and industrial inspection applications [4][5]. Plastic scintillators, due to their inherent characteristics including

low cost, ease of fabrication into large size, desirable environmental stability, and fast scintillation response [6-8], have been frequently used in the field of high-energy physics and in homeland security for gamma counting in radiation portal monitors. Plastic scintillators are readily composed of a polymer matrix (e.g. polystyrene (PS), poly(vinyltoluene) (PVT)), a primary fluorescent dye and a wavelength shifter. Commonly, the scintillation yield of standard organic scintillators is about ten times inferior to the most luminous inorganic scintillators (10,000 ph/MeV vs. 100,000 ph/MeV, respectively), since only the prompt fluorescence resulting from the excitation of singlet states contributes to the yield [9][10].

At present, efforts on utilization of heavy metal organic phosphorescent compounds to enhance quantum efficiency of organic-light-emitting-diode (OLED) devices have led to enormous success, in which both singlet and triplet excitons are harvested [11-14]. Inspired by this idea, Campbell and Crone proposed of doping plastics with iridium(III)tris[2-(4-totyl)pyridinato-NC^2] [$Ir(mppy)_3$] to improve scintillation light yield under ionizing radiation [15]. Plastic scintillators with improved light yield up to 30,000 photons/MeV was achieved in poly(9-vinylcarbazole) utilizing triphenyl bismuth and iridium complex (FIrpic) as dopant by harvesting efficient emission from triplet excitons [16]. The triplet state of iridium was also used as a pulse-shape discriminating (PSD) fast-neutron detector in plastic scintillator [17]. An appropriate selection of the organometallic is needed since some iridium complexes may display undesirable thermoluminescence [18]. In addition to iridium complexes, plastic scintillator films with tris(dibenzoylmethane)mono(1,10-phenanthroline)europium(III) ($Eu[DBM]_3phen$) complex as phosphorescent dopants demonstrate a moderate scintillation yield of 5,650 photons/MeV, but with a penalizing undesired long scintillation decay of 469 μs [19][20]. Thus, an incorporation of organometallic phosphorescent complexes into organic polymer matrix was regarded as an alternative approach to enhance light yield of plastic scintillators.

Recently, quite a few efforts were devoted to finding low-cost metal compounds to replace iridium compounds toward cost-efficient and high-performance luminescence of organocopper complexes or fully organic systems [21-23]. In particular, blue emitting cuprous compounds have attracted extensive attention, and some cuprous compounds have shown thermally activated delayed fluorescence (TADF) and effective singlet emitting in OLEDs [24-26]. Motivated by the excellent performance of Cu(I) complexes as luminescent emitters, the aim of this work is to study the effects of organic copper compounds with high photoluminescence quantum yield (PLQY) on the optical and scintillation properties of plastics for radiation detection applications. Though cuprous compounds can advantageously replace iridium ones in OLED systems, to the best of our knowledge there is only a single publication which reports the use of a chlorine-loaded copper iodide phosphor in a composite scintillator [27].

In this study, $CuI(PPh_3)_2$(*t*-BuPy) (PPh_3 = triphenylphosphine, *t*-BuPy = 4-*tert*-butylpyridine) [28], with deep blue emission and high PLQY up to 100%, is incorporated as the photoluminescent organometallic complex. Transparent plastic scintillators with varying concentrations of $CuI(PPh_3)_2$(*t*-BuPy) from 0.5 to 3 wt% have

been synthesized by bulk polymerization method. To this complex, the 2,5-diphenyloxazole (PPO) and/or 1,4-bis(5-phenyl-2-oxazolyl)benzene (POPOP) were sometimes added. To gain insight into the scintillation mechanism altered by Cu(I) loading complexes, the optical performance, scintillation responses and PSD performance under X-ray, γ-ray and α-particle excitation were systematically investigated.

2. Experimental

2.1 Preparation of plastic scintillators

Vinyltoluene monomer (VT, 98%) was obtained from TCI and purified by silica gel chromatography. Triphenylphosphine (99%), acetonitrile (CH_3CN, 99.9%) were obtained from Adamas. 4-*Tert*-butylpyridine (96%) was obtained from J&K. CuI (99.999%), 1,4-bis[2-(5-phenyloxazolyl)]benzene (POPOP, 99%) and 2,5-diphenyloxazole (PPO, 99%) were obtained from Sigma-Aldrich.

Copper iodide complex $CuI(PPh_3)_2$(*t*-BuPy) was synthesized according to a reported procedure [28]. Synthesized and structural scheme of the $CuI(PPh_3)_2$(*t*-BuPy) complex is presented in **Scheme 1**. The PL, PLE and X-ray excited RL spectra of $CuI(PPh_3)_2$(*t*-BuPy) powder are shown in **Figure S1**. In PL spectrum, upon 365 nm excitation, a deep blue emission band peaking at 460 nm was observed. Its RL emission peaks at 460 nm, which is identical to its PL emission. The optical absorption spectra of $CuI(PPh_3)_2$(*t*-BuPy) in CH_2Cl_2 is shown in **Figure S2**. The bandgap is estimated to be 3.61 eV. It is close to that of PPO about 3.64 eV.

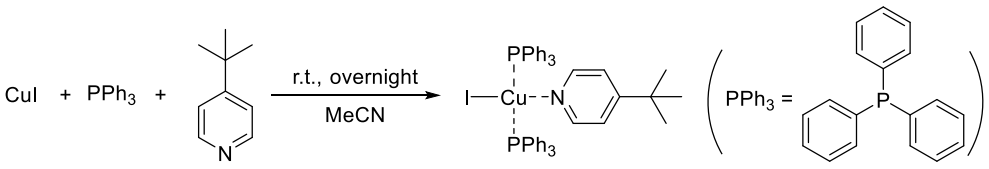

Scheme 1. Synthesis and structure of $CuI(PPh_3)_2$(*t*-BuPy).

Three kind of samples were prepared: 1) VT, the primary fluorescent dye (PPO, 2 wt%), the wavelength shifter (POPOP, 0.1 wt%) and $CuI(PPh_3)_2$(*t*-BuPy) complex at concentrations ranging from 0.5 to 3 wt%; 2) VT, 2 wt% PPO and 2 wt% $CuI(PPh_3)_2$(*t*-BuPy) complex; 3) VT and 2 wt% $CuI(PPh_3)_2$(*t*-BuPy) complex. The mixture was purged with nitrogen, sealed, heated to 80 °C and kept at 80 °C for 3 weeks. Once polymerization was completed, glass containers were slowly cooled to room temperature to reduce internal stress. The size of the obtained samples was 15.5 mm in diameter and 11.0 mm in thickness. They were used for optical absorption, photoluminescence, and scintillation performance evaluation.

2.2 Optical and scintillation property measurements

The optical transmittance and absorption spectra of the polished samples were measured with a PerkinElmer-Lambda 950 UV-VIS-IR spectrophotometer in the wavelength region ranging from 200 nm to 800 nm. Photoluminescence emission (PL)

and excitation (PLE) spectra were acquired by a Horiba Jobin Yvon Fluorolog-3 spectrofluorometer which excitation source is a steady-state Xenon lamp. Time-Resolved Emission Spectroscopy (TRES) measurements were performed with a Horiba Jobin Yvon Fluoromax 4P spectrofluorometer equipped with a 274 nm excitation diode. Elemental analysis was measured by a Hitachi S-4800 scanning electron microscopy with an energy dispersive spectrometer (EDS).

X-ray induced radioluminescence (RL) spectra were obtained by using an X-ray tube operated at 40 kV and 15 mA (Seifert GmbH) as an excitation source in 5000M spectrofluorometer (Horiba Jobin Yvon). Recorded emission spectra were corrected for spectral sensitivity of the detection part.

^{137}Cs (ca. 555 kBq at the time of the experiment) gamma pulse-height spectra were recorded by the set-up consisting of a Hamamatsu R6233-100 PMT operating at -900 V, a Ortec 113 Preamplifier, an Ortec 671 Amplifier, and a Tukan 8k multichannel analyzer. The shaping time was set as 10 μs to ensure full light integration. The samples were directly coupled to the PMT using silicone oil and covered Teflon tape to maximize the collection of light. The pulse height spectra under alpha emitter ^{239}Pu were recorded by the set-up consisting of a Hamamatsu R2048 PMT operating at -800 V. The shaping time was set as 1 μs to ensure full light integration.

The X-ray excited scintillation decays were recorded using a time-correlated single-photon counting setup (Fluorohub electronics coupled with fast hybrid photomultiplier purchased from Horiba Jobin Yvon) under ps X-ray pulse excitation at 40 kV (Hamamatsu). The instrumental response of the set-up was 75 ps.

Alpha/gamma pulse shape discrimination studies were performed using the following experimental setup. The scintillators were optically glued to a R7899 photomultiplier tube (Hamamatsu) operating at negative voltage. The anode fed a DT5730B digitizer (CAEN) which allows both real-time PSD visualization and data post-processing. The scintillator was excited with a ^{244}Cm alpha source in close contact and a ^{60}Co gamma source located approximately 6 cm away from the scintillator.

3. Results and Discussion

3.1 Photophysics and scintillation properties of CuI(PPh_3)$_2$(*t*-BuPy)-loaded PVT/PPO/POPOP plastics

Plastic scintillator samples loaded with different concentrations of CuI(PPh_3)$_2$(*t*-BuPy) ranging from 0 to 3 wt% and containing PPO and POPOP are shown in **Figure 1**. All samples are transparent and colorless under day light and emit bright blue light under UV illumination. Interestingly, in the 3 wt% Cu-complex loaded plastic scintillator the crystallization of precipitates appears during polymerization. The composition of the precipitates was determined by EDS as shown in **Figure S3** and **Table S1**. The atom molar ratio of C: P: I: N: Cu was 85.06: 5.51: 3.29: 3.25: 2.89, which is close to the molar ratio of CuI(PPh_3)$_2$(*t*-BuPy) compound ($C_{45}H_{43}CuINP_2$). It indicates that the precipitates are made from the CuI(PPh_3)$_2$(*t*-BuPy) compound only.

The precipitation most probably occurred due to a thermodynamic solubility limit of CuI(PPh_3)$_2$(*t*-BuPy) in VT than that of in PVT [29].

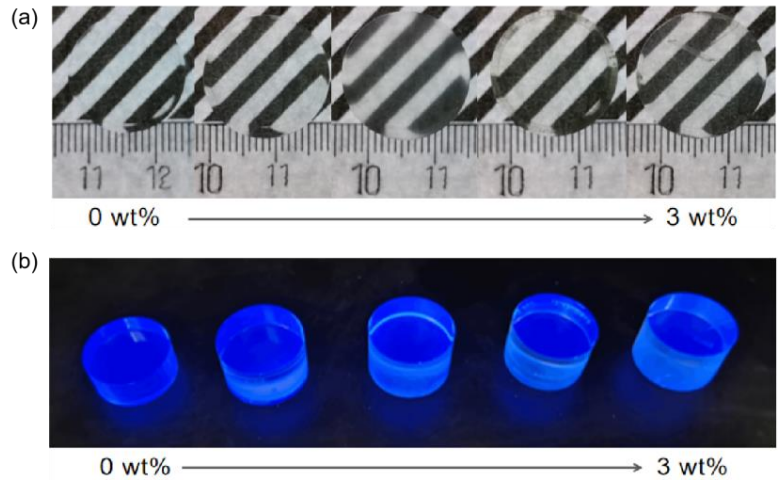

Figure 1. Polished plastic scintillator samples loaded with different concentrations of CuI(PPh_3)$_2$(*t*-BuPy): (a) under day light, (b) under 365 nm UV illumination.

The optical transmittance can directly affect the light yield of plastic scintillation [30]. The optical transmission spectra of unloaded (but still containing PPO and POPOP) and CuI(PPh_3)$_2$(*t*-BuPy)-loaded plastic scintillators are shown in **Figure 2a**. All samples have a high transmittance over 80% above 430 nm. The PL spectra of unloaded and CuI(PPh_3)$_2$(*t*-BuPy)-loaded plastic scintillators have almost the same emission bands peaking at 345, 362, 394, 417, 441 and 462 nm under 320 nm excitation, as shown in **Figure 2b**. The emissions peaking at 345 and 362 nm originate from PPO, and the emissions peaking at 394, 417, 441, and 462 nm originate from POPOP [31]. The PL spectra of unloaded and CuI(PPh_3)$_2$(*t*-BuPy)-loaded plastic scintillators under 365 nm excitation are shown in **Figure S4**. However, the emission from CuI(PPh_3)$_2$(*t*-BuPy) was not observed.

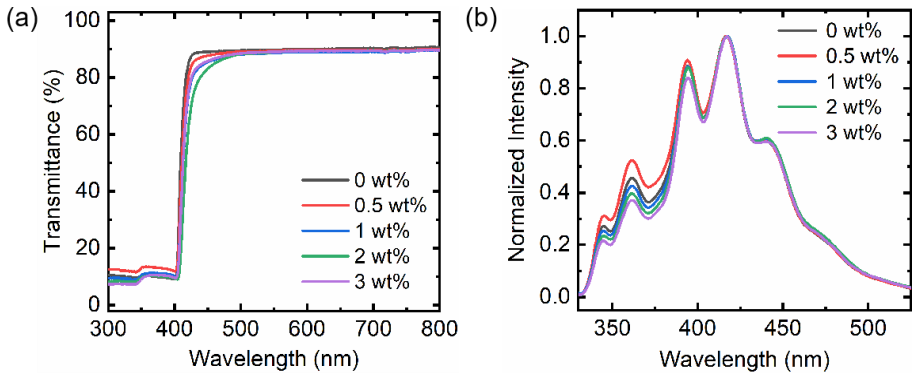

Figure 2. (a) Optical transmission spectra (length 11.0 mm) and (b) PL spectra (λ_{ex} = 320 nm) of CuI(PPh_3)$_2$(*t*-BuPy)-loaded plastic scintillators.

The TRES measurements of the CuI(PPh_3)$_2$(*t*-BuPy)-loaded plastic scintillators under 274 nm excitation are shown in **Figure 3.** We observed weak emission of copper compounds in the 3 wt% CuI(PPh_3)$_2$(*t*-BuPy)-loaded plastic scintillator. In the TRES test results of other samples, we barely observed slow decay from CuI(PPh_3)$_2$(*t*-BuPy), most of which was fast decay signal from fluorescent dyes. It suggests that incorporation of CuI(PPh_3)$_2$(*t*-BuPy) has a small effects on PL performance.

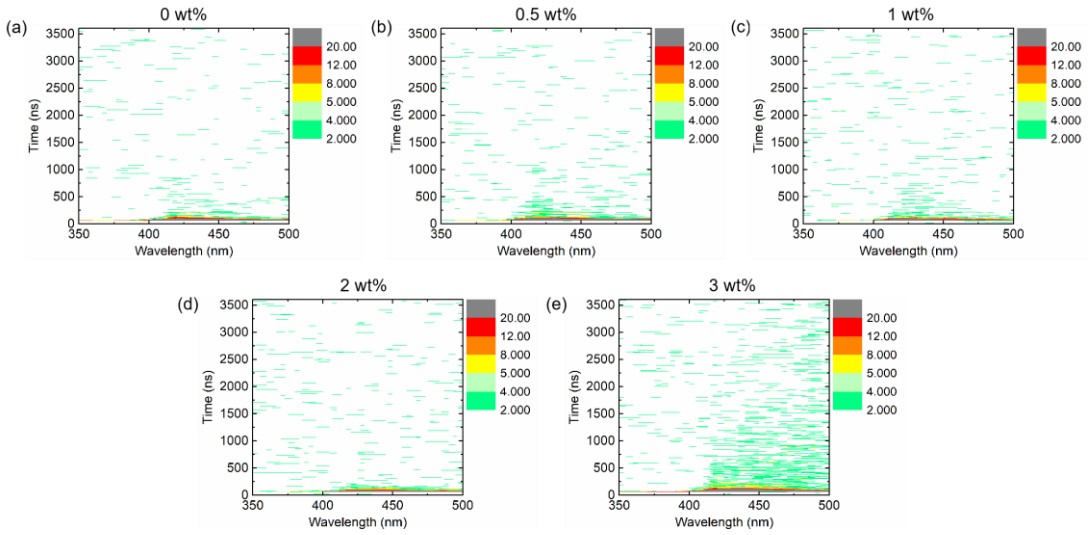

Figure 3. TRES of plastic scintillators loaded with different amounts of CuI(PPh_3)$_2$(*t*-BuPy).

X-ray excited RL spectra of the CuI(PPh_3)$_2$(*t*-BuPy)-loaded plastic scintillators are shown in **Figure 4**. All samples show broad emission bands extending from 390 to 550 nm with maximum at 422 nm, corresponding to the emission of POPOP. Non-existence of PPO emission in RL indicates energy transfer from PPO to POPOP [32]. As shown in **Figure 4a**, the RL integral intensity significantly decreases with the increase of CuI(PPh_3)$_2$(*t*-BuPy) doping concentration. We propose that the RL intensity reduction is related to the self-quenching of CuI(PPh_3)$_2$(*t*-BuPy) due to its aggregation [33],[34].

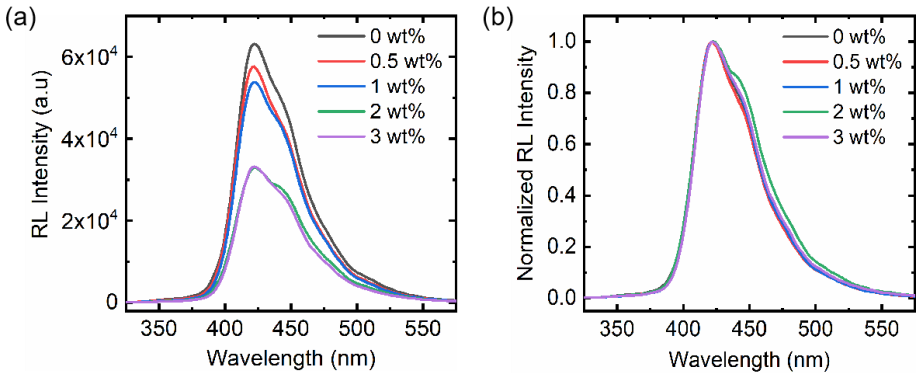

Figure 4. X-ray excited RL spectra of CuI(PPh_3)$_2$(*t*-BuPy)-loaded plastic scintillators.

Scintillation decay measurement can help to evaluate whether CuI(PPh_3)$_2$(*t*-BuPy) compounds actively participate in scintillation emission process [35]. The scintillation

decay profiles of CuI(PPh_3)$_2$(*t*-BuPy)-loaded plastic scintillators were measured under ps X-ray pulse excitation with two different time windows. The instrumental response profile is shown in **Figure S5**. The scintillation decay profiles within 40 ns and 1.2 μs time windows are shown in **Figure 5** and **Figure S6**, respectively. All scintillation decay profiles can be well fitted sum of two-exponentials. As shown in **Figure 5**, the decay time values of CuI(PPh_3)$_2$(*t*-BuPy)-loaded plastic scintillators are notably smaller than that of the unloaded one. The most probable reason is the enhanced probability of non-radiative transition caused by the incorporation of CuI(PPh_3)$_2$(*t*-BuPy). Additionally, there is no slow component even monitoring the μs time scale. All samples have nanosecond decay characteristics of plastic scintillators. It suggests that the fluorescence dye POPOP dominates the scintillation emission process, which is consistent with the result of RL spectra.

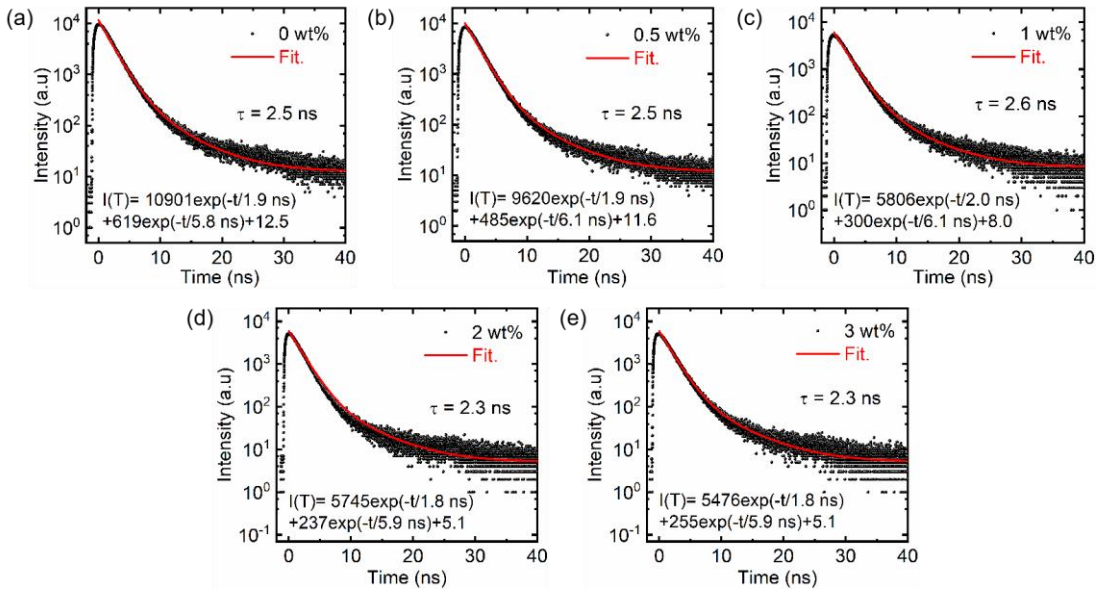

Figure 5. Scintillation decay profiles of CuI(PPh_3)$_2$(*t*-BuPy)-loaded plastic scintillators under ps X-ray pulse excitation.

We further explored the γ-ray response of CuI(PPh_3)$_2$(*t*-BuPy)-loaded plastic scintillators. Pulse height spectra and relative light yield of plastic scintillators with varying concentrations of CuI(PPh_3)$_2$(*t*-BuPy) are plotted in **Figure 6a** and **6b**, respectively. The spectrum of a commercial EJ-200 reference with the same size is also plotted in **Figure 6a** for comparison. The channel number of the middle point where the slope drops to one-half of the Compton edge was used to evaluate the light yield [36]. The light yield significantly decreases from 9300 to 3800 photons/MeV with increasing CuI(PPh_3)$_2$(*t*-BuPy) concentration. The light yield variation trend is consistent with that of steady-state RL emission. In addition, the precipitate which was observed in the 3 wt% loaded plastic gives the same light output of the 2 wt% loaded plastic, reinforcing thus the fact that this precipitate was the copper complex.

Besides X-ray and γ-ray detection performances, scintillation response of CuI(PPh_3)$_2$(*t*-BuPy)-loaded plastic scintillators under alpha particle irradiation was also studied. Pulse height spectra and relative light yield under ^{239}Pu excitation are shown

in **Figure 6c** and **6d**. BGO standard sample has similar diameter as reference, but its thickness is only 1.5 mm. Since the alpha energy is fully released within the scintillator, the maximum of the amplitude of the histogram was considered for light yield calculation. The light yield decreased from 380 to 130 photons/MeV with increasing CuI(PPh_3)$_2$(*t*-BuPy) loading concentration. Again, 2 wt% and 3 wt% loaded samples show the same light output.

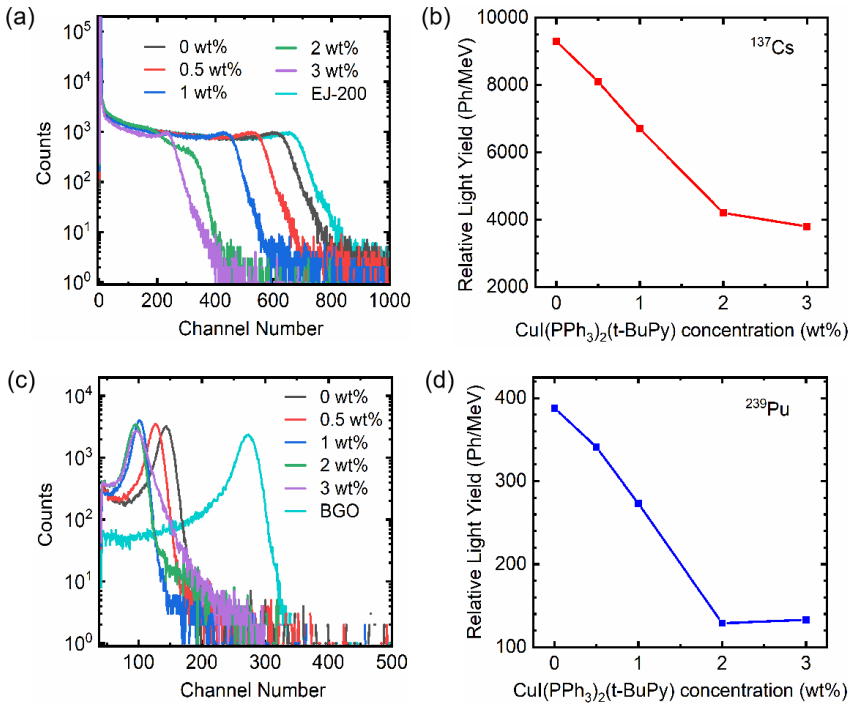

Figure 6. (a) Pulse height spectra and (b) scintillation light yield as a function of CuI(PPh_3)$_2$(*t*-BuPy)-loaded concentration under ^{137}Cs irradiation. (c) Pulse height spectra and (d) scintillation light yield as a function of CuI(PPh_3)$_2$(*t*-BuPy) loaded concentration under ^{239}Pu irradiation.

3.2 Photophysics and scintillation properties of CuI(PPh_3)$_2$(t-BuPy)-loaded PVT and PVT/PPO plastics

To shed light on the mechanism of light yield deterioration, the PVT/2 wt% CuI(PPh_3)$_2$(*t*-BuPy) and PVT/2 wt% CuI(PPh_3)$_2$(*t*-BuPy)/2 wt% PPO plastics were also prepared (see **Figure S7**). The PL and PLE spectra of PVT/2 wt% CuI(PPh_3)$_2$(*t*-BuPy) plastic scintillator are shown in **Figure 7a**. The featured emission at 330 nm associated with PVT is observed under 270 nm excitation, and the featured emission at 520 nm associated with CuI(PPh_3)$_2$(*t*-BuPy) is observed under 350 nm excitation. A large overlap between the emission spectrum of PVT and the excitation spectrum of CuI(PPh_3)$_2$(*t*-BuPy) suggests the existence of energy transfer from PVT to CuI(PPh_3)$_2$(*t*-BuPy). The TRES of PVT/2 wt% CuI(PPh_3)$_2$(*t*-BuPy) plastic scintillator between 350 and 530 nm (274 nm excitation) are shown in **Figure 7b**. With increasing wavelengths, the appearance of the long decay (the orange zone) from CuI(PPh_3)$_2$(*t*-BuPy) over 3500 ns, while the fast decay is always present (the tiny grey line around ordinate 100 ns). The RL spectrum of PVT/2 wt% CuI(PPh_3)$_2$(*t*-BuPy) is shown in

Figure 7c. A broad emission band can be ascribed to emissions from CuI(PPh_3)$_2$(*t*-BuPy).

The PL and PLE spectra of PVT/2 wt% CuI(PPh_3)$_2$(*t*-BuPy)/2 wt% PPO plastic scintillator are shown in **Figure 7d**. The emission of PVT and PPO are observed under 270 nm excitation, and the emission of CuI(PPh_3)$_2$(*t*-BuPy) is observed under 365 nm excitation. There is a considerable overlap between the emission spectrum of PPO and the excitation spectrum of CuI(PPh_3)$_2$(*t*-BuPy). The TRES of PVT/2 wt% CuI(PPh_3)$_2$(*t*-BuPy)/2 wt% PPO plastic scintillator under 274 nm excitation are shown in **Figure 7e**. Compared to PVT/2 wt% CuI(PPh_3)$_2$(*t*-BuPy) plastic scintillator, the incorporation of PPO reduced the long decay ratio (the orange zone reduced). Thus, there is a competition between PPO and CuI(PPh_3)$_2$(*t*-BuPy).The RL spectrum PVT/2 wt% CuI(PPh_3)$_2$(*t*-BuPy)/2 wt% PPO plastic scintillator is shown in **Figure 7f**. A broad emission band shows a maximum at 400 nm (3.1 eV) coming from PPO and an emission peak at 459 nm (2.7 eV) coming from CuI(PPh_3)$_2$(*t*-BuPy). We have also compared the RL intensity under $^{90}Sr/^{90}Y$ radioactive source of 2 wt% CuI(PPh_3)$_2$(*t*-BuPy) loaded samples without or with PPO or POPOP, as shown in **Figure S8**. The RL intensity of sample containing only Cu complex is very low. Therefore, the emission of CuI(PPh_3)$_2$(*t*-BuPy) in plastic scintillators is very weak comparing to PPO and POPOP, which also leads to the reduction of scintillation performance.

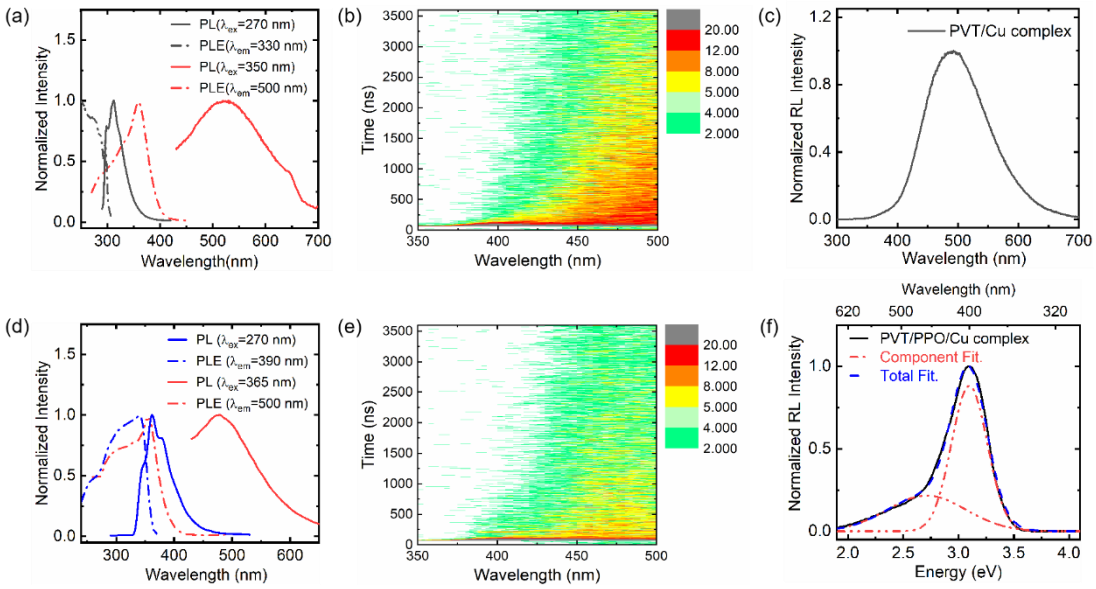

Figure 7. (a) PL and PLE spectra, (b)TRES and (c) X-ray excited RL spectrum of PVT/2 wt% CuI(PPh_3)$_2$(*t*-BuPy) plastic scintillator. (d) PL and PLE spectra, (e)TRES and (f) X-ray excited RL spectrum of PVT/2 wt% CuI(PPh_3)$_2$(*t*-BuPy)/2 wt% PPO plastic scintillator. The fitting curves are also shown.

Combined with the aforementioned results of photoluminescence and scintillation properties, the possible ET paths were proposed in this system (see **Figure 8)**: 1) PVT→PPO→POPOP, 2) PVT→CuI(PPh_3)$_2$(*t*-BuPy), and 3) PVT→PPO→ CuI(PPh_3)$_2$(*t*-BuPy). These three paths are co-existent. In this system, the emission of CuI(PPh_3)$_2$(*t*-BuPy) is very weak, so 2) and 3) ET paths account for energy loss due to the inefficient energy transfer.

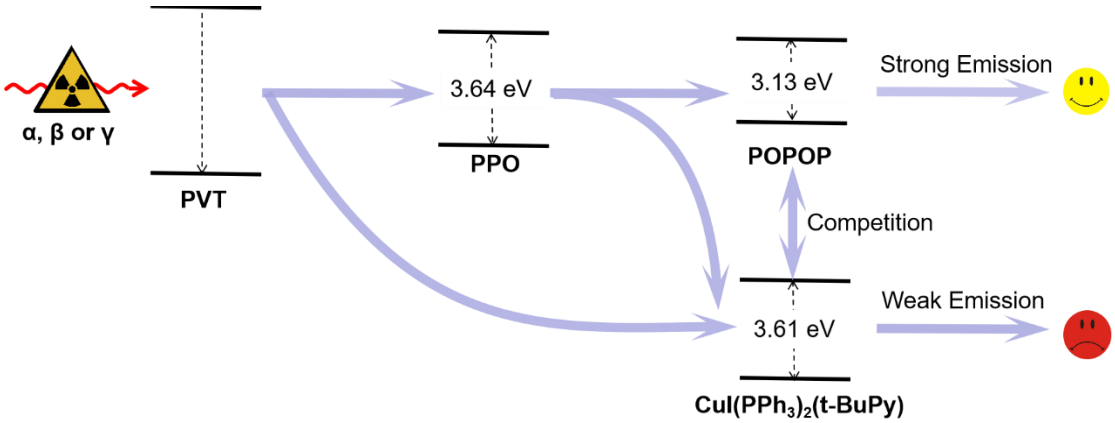

Figure 8. Schematic illustration of energy transfer processes in $CuI(PPh_3)_2$(*t*-BuPy)-loaded PVT plastic scintillators.

3.3 α/γ pulse shape discrimination performances of plastic scintillators

Fig. 9 plots the 2-dimensional α/γ PSD histograms for of (Q_{tail}/Q_{total}) versus Q_{total} for samples of PVT/$CuI(PPh_3)_2$(*t*-BuPy) (Fig. 9(a)) and PVT/PPO/$CuI(PPh_3)_2$(*t*-BuPy) (Fig. 9(b)). One can see the largest difference of the response between (a) and (b), with a strong α/γ discrimination capability for the scintillator based on the copper complex only. This confirms the triplet harvesting capability of the copper complex, a feature which is not possible for PPO.

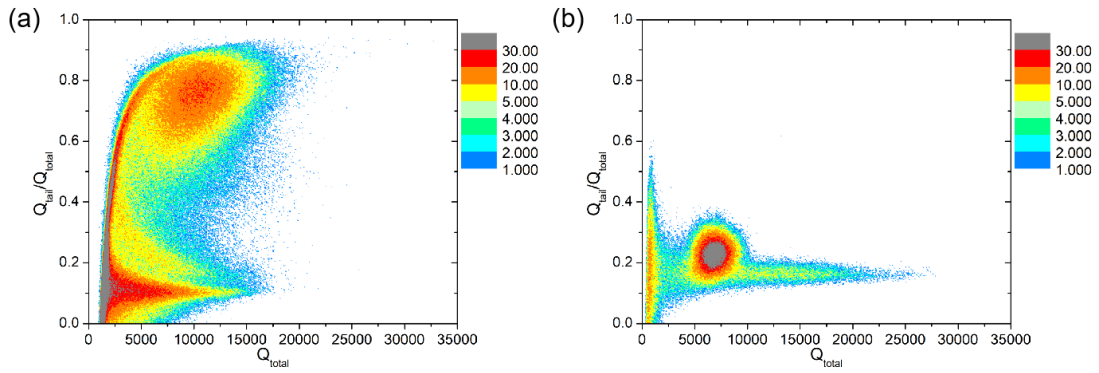

Figure 9. The 2-dimensional α/γ PSD histograms of plastic scintillators (a) with 2 wt% $CuI(PPh_3)_2$(*t*-BuPy) and (b) with 2 wt% $CuI(PPh_3)_2$(*t*-BuPy) and 2 wt% PPO. Note that time gates and photomultiplier gain are not the same for both samples.

4. Conclusion

In summary, high quality polyvinyl toluene-based scintillators loaded with varying $CuI(PPh_3)_2$(*t*-BuPy) concentrations were synthesized. All samples show high optical transmittance over 80% in the concerned wavelength range. The RL emission comes mainly from the singlet state de-excitation of POPOP. The scintillation yield deterioration under X-ray, ^{137}Cs and ^{239}Pu irradiation is probably associated with inefficient energy transfer efficiency from PVT to $CuI(PPh_3)_2$(*t*-BuPy) and from PPO

to $CuI(PPh_3)_2$(*t*-BuPy), and the low efficiency emission of $CuI(PPh_3)_2$(*t*-BuPy). Plastic scintillator containing only $CuI(PPh_3)_2$(*t*-BuPy) also showed α/γ PSD performance. Development of robust and cost-efficient phosphorescent dopants with rigid frame structure and short lifetime to improve light yield is worthy of further investigation.

Declaration of competing interest

The authors declare that they have no known competing financial interests or personal relationships that could have appeared to influence the work reported in this paper.

Acknowledgements

This work was supported by the National Natural Science Foundation of China (grant no. 12005288), the State Key Laboratory of Intense Pulsed Radiation Simulation and Effect (grant no. SKLIPR2119), the State Key Laboratory of Particle Detection and Electronics (grant no. SKLPDE-KF-202112), and the Advance Launch Fund of Science and Technology Innovation Project of Shanghai Institute of Ceramics (2020). Partial support of the Operational Program Research, Development and Education financed by European Structural and Investment Funds and the Czech Ministry of Education, Youth and Sports (Project No. SOLID21 CZ.02.1.01/0.0/0.0/16_019/0000760), and the State Key Laboratory of Intense Pulsed Radiation Simulation and Effect（Project No. SKLIPR2119）is acknowledged.

References

[1] S.W. Moser, W.F. Harder, C.R. Hurlbut, M.R. Kusner, Principles and practice of plastic scintillator design, Radiat. Phys. Chem. 41 (1993) 31–36.

[2] M. Nikl, A. Yoshikawa, Recent R&D Trends in Inorganic Single-Crystal Scintillator Materials for Radiation Detection, Adv. Opt. Mater. 3 (2015) 463–481.

[3] A. Lim, A. Mahl, J. Latta, H.A. Yemam, U. Greife, A. Sellinger, Plastic scintillators with efficient light output and pulse shape discrimination produced via photoinitiated polymerization, J. Appl. Polym. Sci. 136 (2019).

[4] B.D. Milbrath, A.J. Peurrung, M. Bliss, W.J. Weber, Radiation detector materials: An overview, J. Mater. Res. 23 (2008) 2561–2581.

[5] M. Hamel, Plastic Scintillators, Springer International Publishing, Cham, 2021.

[6] M. Watanabe, M. Katsumata, H. Ono, T. Suzuki, H. Miyata, Y. Itoh, K. Ishida, M. Tamura, Y. Yamaguchi, First performance test of newly developed plastic scintillator for radiation detection, Nucl. Instruments Methods Phys. Res. Sect. A Accel. Spectrometers, Detect. Assoc. Equip. 770 (2015) 197–202.

[7] E. van Loef, G. Markosyan, U. Shirwadkar, M. McClish, K. Shah, Gamma-ray spectroscopy and pulse shape discrimination with a plastic scintillator, Nucl. Instruments Methods Phys. Res. Sect. A Accel. Spectrometers, Detect. Assoc. Equip. 788 (2015) 71–72.

[8] E. Saito, H. Miyata, M. Katsumata, Y. Karasawa, T. Koike, H. Ono, M. Watanabe, M. Sato, A. Umeyama, T. Suzuki, M. Tamura, Light yield, long-term stability, and attenuation length

of a new plastic scintillator cured at room temperature, Nucl. Instruments Methods Phys. Res. Sect. A Accel. Spectrometers, Detect. Assoc. Equip. 953 (2020) 162885.

[9] G.H. V Bertrand, M. Hamel, F. Sguerra, Current Status on Plastic Scintillators Modifications, Chem. - A Eur. J. 20 (2014) 15660–15685.

[10] T.J. Hajagos, C. Liu, N.J. Cherepy, Q. Pei, High-Z Sensitized Plastic Scintillators: A Review, Adv. Mater. 30 (2018) 1706956.

[11] M.A. Baldo, M.E. Thompson, S.R. Forrest, High-efficiency fluorescent organic light-emitting devices using a phosphorescent sensitizer, Nature. 403 (2000) 750–753.

[12] C. Adachi, M.A. Baldo, M.E. Thompson, S.R. Forrest, Nearly 100% internal phosphorescence efficiency in an organic light emitting device, J. Appl. Phys. 90 (2001) 5048–5051.

[13] H. Yersin, A.F. Rausch, R. Czerwieniec, T. Hofbeck, T. Fischer, The triplet state of organo-transition metal compounds . Triplet harvesting and singlet harvesting for efficient OLEDs, Coord. Chem. Rev. 255 (2011) 2622–2652.

[14] E. Baranoff, B.F.E. Curchod, FIrpic: Archetypal blue phosphorescent emitter for electroluminescence, Dalt. Trans. 44 (2015) 8318–8329.

[15] I.H. Campbell, B.K. Crone, Efficient plastic scintillators utilizing phosphorescent dopants, Appl. Phys. Lett. 90 (2007) 012117.

[16] B.L. Rupert, N.J. Cherepy, B.W. Sturm, R.D. Sanner, S.A. Payne, Bismuth-loaded plastic scintillators for gamma-ray spectroscopy, EPL (Europhysics Lett. 97 (2012) 22002.

[17] P.L. Feng, J. Villone, K. Hattar, S. Mrowka, B.M. Wong, M.D. Allendorf, F.P. Doty, Spectral- and Pulse-Shape Discrimination in Triplet-Harvesting Plastic Scintillators, IEEE Trans. Nucl. Sci. 59 (2012) 3312–3319.

[18] F. Sguerra, R. Marion, G.H. V. Bertrand, R. Coulon, É. Sauvageot, R. Daniellou, J.-L. Renaud, S. Gaillard, M. Hamel, Thermo- and radioluminescent polystyrene based plastic scintillators doped with phosphorescent iridium(III) complexes, J. Mater. Chem. C. 2 (2014) 6125.

[19] A.F. Adadurov, P.N. Zhmurin, V.N. Lebedev, V.V. Kovalenko, Plastic scintillator with phosphorescent dopants for α-particles registration, Nucl. Instruments Methods Phys. Res. Sect. A Accel. Spectrometers, Detect. Assoc. Equip. 621 (2010) 354–357.

[20] A.F. Adadurov, P.N. Zhmurin, V.N. Lebedev, V.N. Kovalenko, Plastic scintillators with β-diketone Eu complexes for high ionizing radiation detection, Appl. Radiat. Isot. 69 (2011) 1475–1478.

[21] C. Torres Ziegenbein, S. Fröbel, M. Glöß, R.S. Nobuyasu, P. Data, A. Monkman, P. Gilch, Triplet Harvesting with a Simple Aromatic Carbonyl, ChemPhysChem. 18 (2017) 2314–2317.

[22] B. Huitorel, H. El Moll, R. Utrera-Melero, M. Cordier, A. Fargues, A. Garcia, F. Massuyeau, C. Martineau-Corcos, F. Fayon, A. Rakhmatullin, S. Kahlal, J.-Y. Saillard, T. Gacoin, S. Perruchas, Evaluation of Ligands Effect on the Photophysical Properties of Copper Iodide Clusters, Inorg. Chem. 57 (2018) 4328–4339.

[23] M. Elie, F. Sguerra, F. Di Meo, M.D. Weber, R. Marion, A. Grimault, J. Lohier, A. Stallivieri, A. Brosseau, R.B. Pansu, J. Renaud, M. Linares, M. Hamel, R.D. Costa, S. Gaillard, Designing NHC–Copper(I) Dipyridylamine Complexes for Blue Light-Emitting Electrochemical Cells, ACS Appl. Mater. Interfaces. 8 (2016) 14678–14691.

[24] R. Czerwieniec, J. Yu, H. Yersin, Blue-Light Emission of Cu(I) Complexes and Singlet Harvesting, Inorg. Chem. 50 (2011) 8293–8301.

[25] J. Egly, D. Bissessar, T. Achard, B. Heinrich, P. Steffanut, M. Mauro, S. Bellemin-Laponnaz, Copper(I) complexes with remotely functionalized phosphine ligands: Synthesis, structural variety, photophysics and effect onto the optical properties, Inorganica Chim. Acta. 514 (2021) 119971.

[26] X.-L. Chen, R. Yu, Q.-K. Zhang, L.-J. Zhou, X.-Y. Wu, Q. Zhang, C.-Z. Lu, Rational Design of Strongly Blue-Emitting Cuprous Complexes with Thermally Activated Delayed Fluorescence and Application in Solution-Processed OLEDs, Chem. Mater. 25 (2013) 3910–3920.

[27] S. Hao, X. Liu, M. Gu, Q. Li, M. Huang, H. Yang, Development of CuI:Cl-PS composite scintillator, J. Lumin. (2021) 118449.

[28] L. Wang, Y. Guo, B. Yu, W. Zhang, T. Li, J. Qu, Simple cuprous iodide complex-based crystals with deep blue emission and high photoluminescence quantum yield up to 100%, Appl. Organomet. Chem. 33 (2019) e4731.

[29] T.J. Hajagos, D. Kishpaugh, Q. Pei, Pulse shape discrimination properties of plastic scintillators incorporating a rationally designed highly soluble and polymerizable derivative of 9,10-diphenylanthracene, Nucl. Instruments Methods Phys. Res. Sect. A Accel. Spectrometers, Detect. Assoc. Equip. 825 (2016) 40–50.

[30] J. Zhu, Y. Ding, J. Zhu, D. Qi, M. Su, Y. Xu, Y. Bi, R. Lin, L. Zhang, Preparation and characterization of a novel UV-curable plastic scintillator, Nucl. Instruments Methods Phys. Res. Sect. A Accel. Spectrometers, Detect. Assoc. Equip. 817 (2016) 30–34.

[31] Y. Xu, H. Deng, H. Lei, G. Chang, Initiator-free preparation and properties of polystyrene-based plastic scintillators, J. Polym. Res. 26 (2019) 177.

[32] H. Zhao, H. Yu, C. Redding, Z. Li, T. Chen, Y. Meng, T.J. Hajagos, J.P. Hayward, Q. Pei, Scintillation Liquids Loaded with Hafnium Oxide Nanoparticles for Spectral Resolution of γ Rays, ACS Appl. Nano Mater. 4 (2021) 1220–1227.

[33] W. Holzer, A. Penzkofer, T. Tsuboi, Absorption and emission spectroscopic characterization of $Ir(ppy)_3$, Chem. Phys. 308 (2005) 93–102.

[34] X. Wang, H. Shi, H. Ma, W. Ye, L. Song, J. Zan, X. Yao, X. Ou, G. Yang, Z. Zhao, M. Singh, C. Lin, H. Wang, W. Jia, Q. Wang, J. Zhi, C. Dong, X. Jiang, Y. Tang, X. Xie, Y. (Michael) Yang, J. Wang, Q. Chen, Y. Wang, H. Yang, G. Zhang, Z. An, X. Liu, W. Huang, Organic phosphors with bright triplet excitons for efficient X-ray-excited luminescence, Nat. Photonics. 15 (2021) 187–192.

[35] T. Chen, H. Yu, X. Wen, C. Redding, T.J. Hajagos, H. Zhao, J.P. Hayward, C. Yang, Q. Pei, A Plastic Scintillator Based on an Efficient Thermally Activated Delayed Fluorescence Emitter 9-(4-(4,6-diphenyl-1,3,5-triazin-2-yl)-2-methylphenyl)-3,6-dioctyl-9H-carbazole for Pulse Shape Discrimination Measurement, Adv. Opt. Mater. 9 (2021) 2001975.

[36] C.H. Lee, J. Son, T.-H. Kim, Y.K. Kim, Characteristics of Plastic Scintillators Fabricated by a Polymerization Reaction, Nucl. Eng. Technol. 49 (2017) 592–597.